Decreasing photobleaching by silver nanoparticles on metal surfaces: application to muscle myofibrils

Priya Muthu
Ignacy Gryczynski
Zygmunt Gryczynski
John M. Talent
Irina Akopova
Julian Borejdo
University of North Texas Health Science Center
Department of Molecular Biology and Immunology
Department of Cell Biology and Genetics
Center for Commercialization of Fluorescent Technology
Fort Worth, Texas 76107
E-mail: jborejdo@hsc.unt.edu

Abstract. Recently it has become possible to study single protein molecules in a cell. However, such experiments are plagued by rapid photobleaching. We recently showed that the interaction of fluorophores with localized surface plasmon polaritons (LSPs) induced in the metallic nanoparticles led to a substantial reduction of photobleaching. We now investigate whether the photobleaching could be further reduced when the excited fluorophore interacts with the LSP excited in the metallic nanoparticles resident on mirrored surface. As an example we use myofibrils, subcellular structures within skeletal muscle. We compare nanoparticle-enhanced fluorescence of myofibrils in the presence and in the absence of a mirrored surface. The proximity of the mirrored surface led to enhancement of fluorescence and to a decrease in fluorescent lifetime, much greater than that observed in the presence of nanoparticles alone. We think that the effect is caused by the near-field interactions between fluorophores and LSP, and between fluorophores and propagating surface plasmons (PSPs) produced in the metallic surface by the nanoparticles. Photobleaching is decreased because fluorescence enhancement enables illumination with a weaker laser beam and because the decrease in fluorescence lifetime minimizes the probability of oxygen attack during the time a molecule is in the exited state. © *2008 Society of Photo-Optical Instrumentation Engineers.* [DOI: 10.1117/1.2854120]

Keywords: photobleaching; surface plasmons.

1 Introduction

The study of single protein molecules in a cell avoids the problems associated with averaging responses from an assembly of molecules with different kinetics and the problems of crowding of proteins in a cell. However, it requires that the data be collected from a small enough volume, and that photobleaching be reduced.

The volume must be small enough to contain a single molecule, which means that it must be subfemtoliter. We recently showed that it is possible to reduce the detection volume far beyond that which is feasible with confocal or even total internal reflection fluorescent microscopy (TIRFM) by coupling excitation and emission light to propagating surface plasmons (PSPs). PSPs are propagating charge density oscillations induced by light impinging on the metal surface at the surface plasmon resonance (SPR) angle. The resulting surface-plasmon-assisted microscope[1,2] (SPAM) reduced the detection volume to a few attoliters (10^{-18} L), making it possible to detect single cross-bridges in a skeletal muscle myofibril.[2]

The photobleaching arises because signal from a single molecule must be measured with a high signal-to-noise ratio (SNR). This requires that the rate of photon detection per molecule be high and necessitates illuminating a sample with an intense laser beam. This, in turn, leads to rapid photobleaching of the fluorophores labeling proteins. Unlike photobleaching of fluorophores in solution or in membranes, where bleached-out molecules are replenished by diffusion,[3] photobleaching of immobile fluorophores is particularly severe.[2] Adding oxygen scavenging reagents to the sample medium[4] alleviates the problem only marginally.

In an earlier work,[5] we were able to decrease photobleaching by taking advantage of the well-known phenomenon that a fine metallic nanoparticle can support localized surface plasmon (LSP) polariton modes (charge density oscillations confined to nanoparticles[6]). Exciting LSPs by light of appropriate wavelength caused the appearance of the plasmon absorption bands and a strong enhancement of the local electric field, resulting in stronger fluorescence signal in surface immunoassays.[7] [It also results in a strong light scattering, which is responsible for the intense red color of aqueous dispersions of colloidal gold particles[8] (*aurum potabilis*)]. This enhancement enables a significant reduction of the excitation intensity. In addition, a decrease in the fluorescence lifetime caused by the distance-dependent changes in the radiative decay rates[9] significantly reduced the rate of photobleaching of rhodamine dye attached to thin filaments of skeletal muscle myofibrils.[5] Specifically, when the metallic nanoparticles were

Address all correspondence to Julian Borejdo, Mol Biol, University of North Texas HSC, 3500 Camp Bowie Blvd, Fort Worth, TX 76107; Tel: 817 735 2106; Fax: 817-735-2118; E-mail: jborejdo@hsc.unt.edu

in the form of silver island films[10–16] (SIFs), the intensity of rhodamine fluorescence increased four- to fivefold and the fluorescence lifetime decreased, on average, 23-fold. As a consequence, the rate of photobleaching of rhodamine-actin in a myofibril placed on glass coverslips coated with SIF decreased ~ twofold in comparison with photobleaching of myofibrils placed on uncoated coverslips.

In this paper, we report a more advanced attempt to decrease bleaching by exciting the LSP modes in SIFs and PSPs on a mirrored surface. The coupling of LSPs with PSPs reduces photobleaching more effectively than SIFs on plain glass and thus should make a significant difference to the feasibility of single-molecule detection (SMD). We used skeletal muscle myofibrils as a model system. Myofibrils are ~10-μm-long, ~0.5-μm-wide, and ~200-nm-thick subcellular structures that are made by homogenizing skeletal muscle at high rate of shear. They contain actin in the form of ~1-μm-long thin filaments, each of which contains ~400 actin protomers. These protomers were labeled with rhodamine. We excited LSPs by illuminating myofibrils on mirrors, using a configuration in which a sample in an aqueous medium is illuminated directly by the laser beam and radiates into a high-refractive-index medium.[12,13,15–17] This mode of illumination sidesteps the difficulty that the substrate is very opaque (it consists of both the mirror and SIFs). PSPs were excited in the metallic surface by SIF nanoparticles. This configuration led to a significant enhancement of fluorescence and to a large decrease in fluorescent lifetime. The mechanism of this process is unclear. We think that the effect is caused both by (1) reflection from the mirror and (2) greatly enhanced near-field dipole-dipole coupling interaction between LSPs and PSPs on the metallic surface, which can lead to a significant increase of the spontaneous emission rate of a fluorophore. Field enhancement led to an increase of brightness, which decreased photobleaching because it enabled illumination with a weaker laser beam. The presence of mirrored substrates significantly decreased the lifetime of the SIF-enhanced fluorescence of rhodamine myofibrils. This decrease in lifetime reduced photobleaching because it minimized the probability of oxygen attack during the time a fluorescent molecule was in the exited state. Both fluorescence enhancement and lifetime decrease were greater than the ones observed when only PSP (Ref. 2) or LSP modes (Ref. 5) were excited. Bleaching of myofibrils placed on silver mirrors and coated with SIFs decreased by a factor of ~3, making it feasible to measure the signal of a single cross-bridge within a muscle sarcomere.

2 Materials and Methods

2.1 Chemicals and Solutions

The fluorescein-phalloidin, unlabeled phalloidin, phosphocreatine, creatine kinase, glucose oxidase, and catalase were from Sigma (St Louis, Missouri). The rhodamine-phalloidin was from Molecular Probes (Eugene, Oregon).

2.2 Preparation of Myofibrils

Rabbit psoas muscle was first prewashed with cold EDTA-rigor solution (50 mM KCl, 2 mM EDTA, 10 mM DTT, and 10 mM TRIS-HCl pH 7.6) for $\frac{1}{2}$ h, followed by Ca-rigor solution (50 mM KCl, 2 mM MgCl$_2$, 0.1 mM CaCl$_2$, 10 mM DTT, and 10 mM TRIS-HCl pH 7.6). Myofibrils were made from muscle as previously described.[2]

2.3 Labeling and Preparation of Myofibrils

Unless otherwise indicated, myofibrils (1 mg/mL) on glass coverslips were labeled for 5 min with 0.01 μM fluorescent phalloidin (RP)+9.99 μM unlabeled phalloidin (UP). When indicated, they were labeled for 5 min with 0.1 μM RP +9.9 μM UP. After labeling, myofibrils were washed by centrifugation on a desktop centrifuge at 3000 rpm for 2 min followed by resuspension in rigor solution. Myofibrillar suspension (15 μL) was placed on uncoated or coated coverslips then covered with glass coverslip (to avoid drying); and washed with three to four volumes of rigor solution containing phosphocreatine, creatine kinase, glucose oxidase and catalase to remove oxygen.[4]

2.4 Microscope Slides

Microscope slides were covered with metal by vapor deposition by EMF Corp. (Ithaca, New York). A 52-nm-thick layer of silver, a 48-nm layer of gold, or a 20-nm layer of aluminum was deposited on the slides. A 2-nm chromium undercoat was used as an adhesive background. A 5-nm layer of silica was layered on top of the silver, to protect it from oxidation by air.

2.5 Preparation of Silver Island Films

Slides were incubated with poly-L-lysine solution (Sigma, 0.1%) for 1 h and rinsed thoroughly with water. Then 500 mg of AgNO$_3$ (99%, Aldrich) was dissolved in 60 ml of water and 5% NaOH was added until a brown precipitate developed. The precipitate was collected, redissolved by the addition of 30% NH$_4$OH, and then cooled in ice for 3 min. Next, 15 ml of glucose (48 mg/ml) were added to this solution and the coverslips were inserted into it. The solution was then heated for 2 min, followed by cooling at room temperature (RT) for 3 min. The slides were removed when the solution turned cloudy.

2.6 Data Analysis

Data were processed using MathCad 2001i Professional.

2.7 Atomic Force Microscope (AFM)

Imaging was performed on the AFM Explorer (ThermoMicroscopes/Veeco Instruments Inc.) in contact scanning mode with a Non-Conductive Silicon Nitride Probe (Veeco Instruments Inc.). Images were acquired at a rate of 2 to 5 μm/s with a resolution of 300 pixels/line. Images were then processed with WSxM Version 4.0 software for 3-D structure and analyzed with the Veeco SPMLab Version 6.0.2 software for Z, X, and Y distance quantification.

2.8 Bulk Fluorescence Measurements

The sample was positioned in the sample compartment of a Varian Eclipse Spectrofluorometer (Varian, Inc.) in the front-face configuration. The excitation was at 475 nm, and on the
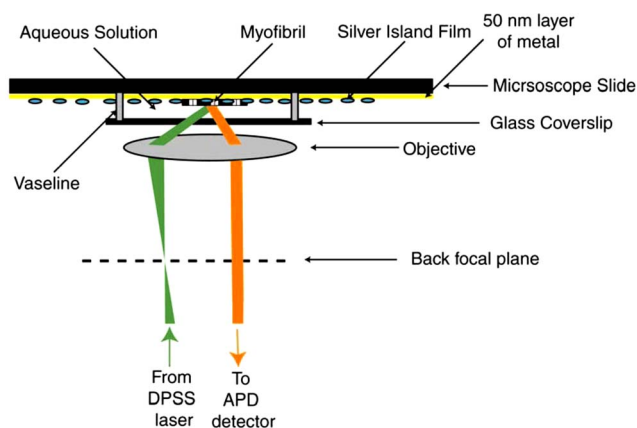
Fig. 1 Experimental arrangement. Myofibril is placed on microscope slide covered with thin layer of metal and coated with SIF. An experimental chamber is made by covering a sample with a glass coverslip. The sample is illuminated directly by the green light, not necessarily at a total internal reflection fluorescent (TIRF) angle, because the evanescent wave produced at the coverslip/buffer interface does not reach a sample in any case. Fluorescence (orange) is collected by the objective, projected by the tube lens onto a confocal aperture, and detected by the APD.

observation we used a 540-nm-long wave pass filter. Under these conditions, there was no detectable signal from bare glass slide or SIF reference slide.

2.9 Measuring Fluorescence Lifetimes

Fluorescence lifetimes were measured by the time-domain technique using FluoTime 200 fluorometer (PicoQuant, Inc.). The sample was positioned in front-face configuration inside the fluorometer chamber. The excitation was by a 475-nm laser-pulsed diode, and the observation was through a monochromator at 575 nm with a supporting 550-nm-long wave pass filter. The FWHM of pulse response function was 68 ps (measured by PicoQuant, Inc.). The reconvolution procedure was used to take into account the excitation pulse shape. The time resolution was better than 10 ps. Less than 0.5% background was detected from the SIF slide. The intensity decays were analyzed in terms of a multiexponential model using FluoFit software (PicoQuant, Inc.).

2.10 Microscopic Measurements

The microscope was described earlier.[18] Here we used a modification whereby the myofibril is first placed on a metal-covered microscope slide coated with SIF and then immersed in Ca-rigor solution. A small chamber was made by sealing the sides around the sample with Vaseline and the top with a #1 glass coverslip (Fisher) (Fig. 1). The chamber is placed coverslip-down on a movable piezostage (Nano-H100, Mad City Labs, Madison, Wisconsin) that is installed on the stage of an Olympus $I \times 51$ microscope. The piezostage is controlled by a nanodrive. This provides sufficient resolution to place the region of interest (ROI) in a position conjugate to the confocal aperture.[19] The excitation light from an expanded diode-pumped solid state (DPSS) laser beam (Compass 215M, Coherent, Santa Clara, California) enters the commercial TIRF illuminator (Olympus, Center Valley, Pennsylva-

nia). The expanded laser beam is focused at the back focal plane of the objective and directed by the movable optical fiber adapter to the periphery of the objective [Olympus PlanApo $60\times$, 1.45 numerical aperture (NA)]. At the interface between glass and solution the beam refracts and propagates toward the sample at an acute incidence angle. Note that this angle is not equal to the TIRF angle. TIRF excitation is impossible with this configuration, because the evanescent wave, which is created at the glass-solution interface, never reaches the muscle. The sample is excited directly by the laser beam, not by evanescent wave. The same NA=1.45 objective is used to collect the fluorescent light. The light is projected onto a tube lens, which focuses it at the conjugate image plane. A confocal aperture or an optical fiber (whose core acts as a confocal aperture) is inserted at this plane. An avalanche photodiode (APD, Perkin-Elmer SPCM-AQR-15-FC) collects light emerging from the aperture.

The conditions of the intensity measurements on different substrates were kept strictly the same. The samples were placed sequentially on the microscope stage without altering the focus or angle of illumination. The nature of the metal substrate did not affect the focus. The angle of illumination was unchanged, since samples were not illuminated by TIRF. The only modification allowed was insertion of neutral density filters in the excitation light path. This was necessary because the APD was becoming saturated when measuring fluorescence on highly enhancing substrates (e.g., silver +SIF). The values reported are those obtained within first few seconds after opening the shutter and admitting laser light.

2.11 Selecting Aperture Size

The projection of the aperture on the object plane defines the lateral (X, Y) dimension of the detection volume, and is equal to the diameter of the confocal aperture (D) divided by the magnification of the objective $(M=60)$. The aperture should be as large as possible to maximize the signal, but it makes no sense to make the projection less than $R=0.25$ μm, the optical resolution of the NA=1.45 objective used here. Therefore, the optimal size of the confocal aperture is $D=MR=15$ μm. Since there are no commercial optical fibers of this size, we used 4-μm fibers.

2.12 Number of Observed Molecules

The detection volume is $\pi(D/2)^2 H$, where H is the height of the volume. Since we did not use TIRF illumination, $H=$ ~ 100 nm (the average thickness of a myofibril, see Fig. 2), and the detection volume is $\sim 20 \times 10^{-18}$ L. Actin concentration in muscle (0.6 mM) implies that there are ~ 7200 actin protomers in this volume. The ratio of fluorescent phalloidin to nonfluorescent phalloidin was fixed at 1:1000, suggesting that the signal was contributed on average by about seven to eight actin molecules.

3 Results

3.1 AFM Images of Surfaces

Figure 2 shows representative AFM images of [Fig. 2(A)] a silver mirror, [Fig. 2(B)] a silver mirror coated with SIF, and [Fig. 2(C)] myofibrils on silver mirror coated with SIF. All images are 10×10 μm. The peaks in the southwest corner of
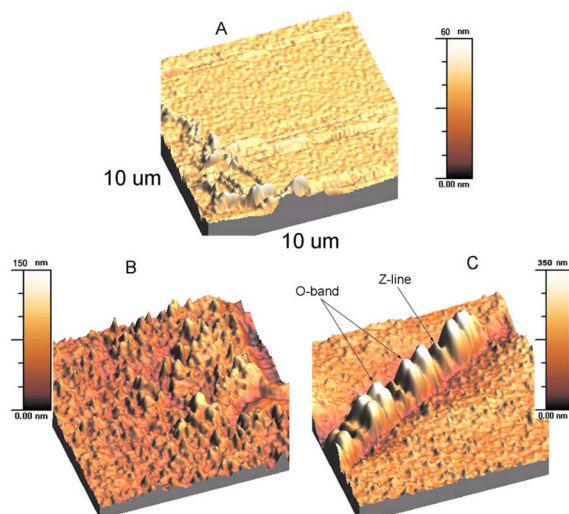
Fig. 2 (a) AFM image of a glass coverslip covered with silver, (b) glass coverslip covered with silver and coated with SIF, and (c) myofibrils on the glass coverslip covered with silver and coated with SIF. All images are 10×10 μm. The peaks in the southwest corner of (a) are dirt particles. The dirt is present because the slides initially contained aqueous buffer. They were used in experiments, dried, and AFM imaged.

Fig. 2(A) are dirt particles. The 52-nm layer of silver was protected by a 5-nm coat of silica, which was responsible for small "bumps" present in Figs. 2(B) and 2(C). The average diameter of SIF was 217 ± 22 nm [mean $\pm$ standard deviation (SD)]. We think that the area of a sarcomere projecting above the surface of the coverslip in Fig. 2(C) is the O-band, because it is offering more resistance to the AFM probe as a consequence of having been strengthened by the attachment of phalloidin. The thickness of myofibrils was calculated from AFM images by measuring the distance from the coverglass to the highest point of elevation of the O-band. In 12 measurements on phalloidin-labeled myofibrils, the average height of a myofibril was 97 ± 4 nm. The average width was 1.68 ± 0.44 μm (mean+SD). It is clear that the average height of a myofibril is smaller than the $1/e$ distance of an evanescent wave, and therefore there is no advantage to TIRF illumination.

3.2 Increase of Brightness

Figure 3 compares the spectra of myofibrils on glass coverslips coated with SIF with the spectra of myofibrils on silver mirror coated with SIF. The emission spectra were recorded in a Cary Eclipse spectrofluorometer by placing the plane of the microscope slide at a 45-deg angle with respect to the direction of the exciting 475-nm beam of light. No differences in the shape of emission spectra were detected, but the intensity of fluorescence of myofibrils on glass+SIF was enhanced $\sim 3.6 \pm 0.2$ times (mean $\pm$ SE) by the silver mirror in comparison with the intensity of myofibrils on glass alone. Gold and aluminum enhanced the fluorescence by a factor of 4 (Table 1, column 2). This effect is caused by the presence of the mirror surface, which enhances intensity by a trivial reflection from the reflecting surface. The reflection enhances both illuminating light fluxes (the sample is illuminated di-
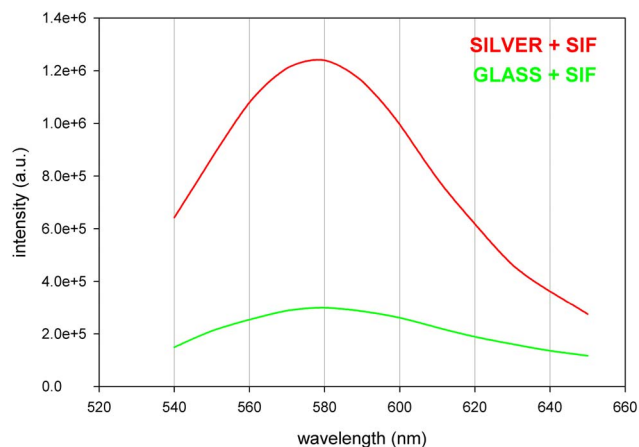

Fig. 3 Enhancement of fluorescence by SIF on silver. Myofibrils (1 mg/mL) labeled with 0.1 μM Rh-phalloidin were placed on a glass coverslip coated with SIF (green) and on a glass covered with silver and then coated with SIF (red). The spectra were measured at a 45 deg angle in a Varian Eclipse spectrofluorometer. The excitation wavelength is 475 nm. The vertical scale is in arbitrary units (a.u.). The spectrum of SIF in the absence of muscle is less than 10 a.u. at all wavelengths. (Color online only.)

rectly, and the fluorescent light is reflected from the surface). SIF alone (no mirror) enhanced[5] intensity by a factor of 4 to 5. The increases in intensities of myofibrils on metal coated glass in the presence of SIF are listed in Table 1 (column 3). The strongest enhancement in fluorescence signal was observed for the SIF deposited on silver mirror, which is consistent with earlier report on enhanced immunoassays.[7] Intrigued by the high magnitude of the observed enhancements on the metallic surfaces coated with nanoparticles, we decided to study this effect in more detail, exploring the changes in lifetimes and photostabilities.

3.3 Decrease of Fluorescent Lifetime

To quantify the effect of SIF, we measured the lifetimes of myofibrils on various metallic surfaces. The results show that the fluorescence lifetime is decreased with a simultaneous increase of the brightness. This suggests that the proximity of fluorophores to metallic surfaces increased the radiative rate because the decrease of lifetime is the distinguishing feature of the increase of radiative rate.[20] The observed decrease of the lifetime cannot be solely a result of the increase in the

Table 1 Enhancement of fluorescence intensity of phalloidin labeled myofibrils with reference to glass alone (column 1) by the mirrored surface alone (column 2), and the mirror together with SIF (column 3).

Glass	Glass+Me	Glass+Me+SIF
1	4 (Au)	10 ± 0.0 (Au)
1	3.6 (Ag)	259 ± 50 (Ag)
1	4 (Al)	13.2 ± 0.8 (Al)

SIF alone with no mirror gave a four- to fivefold enhancement. The metal is identified in the brackets.
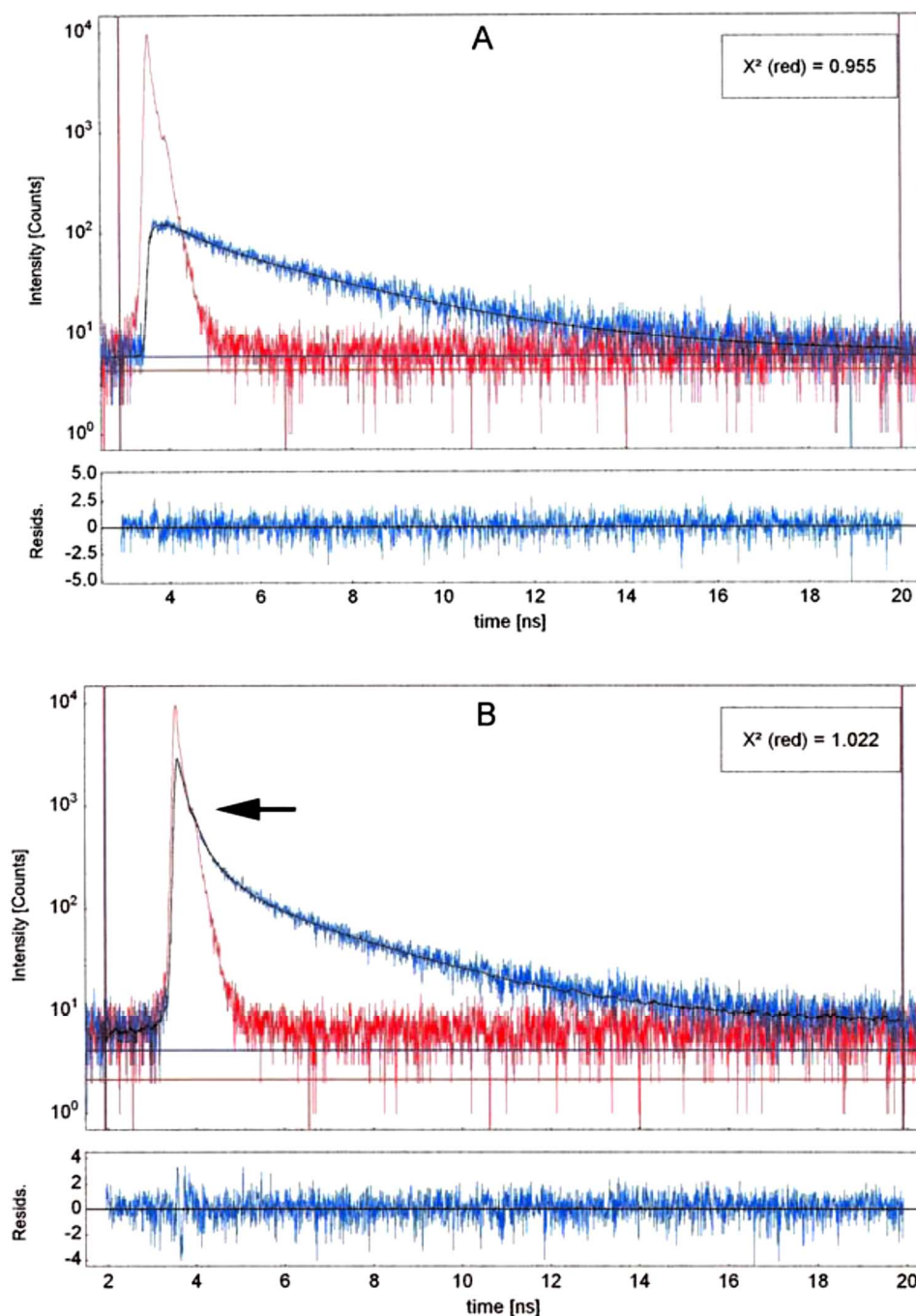
Fig. 4 Decrease of lifetime caused by SIF. (a) Lifetime signal from myofibrils on glass (blue) is best fitted (black line) by the two exponentials with lifetimes $\tau_1 = 0.60$ and $\tau_2 = 3.18$ ns and the relative contributions to the total amplitude of 41.81 and 58.19%. The red signal is the exciting pulse from the diode laser. The bottom inset is the residual fit to all 2134 analyzed data points. (b) Lifetime signal from myofibrils on glass coated with SIF (blue) is best fitted (black line) by three exponentials with lifetimes $\tau_1 = 2.775$, $\tau_2 = 0.544$, and $\tau_3 = 0.063$ ns and with the relative contributions to the total amplitude of 1.51, 4.28, and 94.20%. The arrow points to the fast decay of fluorescence. The red signal is the exciting pulse. The bottom inset is the residual fit to all 2245 data analyzed points. (Color online only.)

nonradiative rate because the quantum efficiency is also increased, and any increase in nonradiative rate decreases the brightness.

3.3.1 GLASS+SIF

Figure 4 shows that SIF causes the fluorescent lifetime to significantly decrease. The decay of fluorescence of myo-

fibrils on glass [Fig. 4(A) and Table 2] was best fitted by two exponentials with lifetimes $\tau_1 = 0.60 \pm 0.14$ and $\tau_2 = 3.18 \pm 0.12$ ns with the relative contributions to the total amplitude of 41.81 and 58.19%, respectively. The amplitude weighted average lifetime was 2.100 ns. Addition of SIF [Fig. 4(b)] augmented the fast decay of fluorescence of myofibrils (arrow). It was now best fitted by three exponentials with

Table 2 Effect of SIF on different surfaces on the amplitude-weighted component of the fluorescence lifetime of phalloidin.

Substrate	Lifetime in the Absence of SIF (ns)	Lifetime in the Presence of SIF (ns)	Decrease (fold)
Glass	2.100	0.125	16.8
Ag	2.328	0.068	34.2

lifetimes $\tau_1=2.775\pm0.082$, $\tau_2=0.544\pm0.033$, and $\tau_3=0.063\pm0.0018$ ns with the relative contributions to the total amplitude of 1.51, 4.28, and 94.20%, respectively. The amplitude weighted average lifetime decreased nearly 17 times to 0.125 ns.

3.3.2 Silver+SIF

Figure 5(A) shows that the decay of fluorescence of myofibrils on silver mirrors was best fitted by two exponentials with lifetimes $\tau_1=0.936\pm0.064$ and $\tau_2=3.380\pm0.041$ ns with the relative contributions to the total amplitude of 43.05 and 56.95%, respectively (Table 2). The amplitude-weighted average lifetime was 2.328 ns. Figure 5(B) shows that addition of SIF augmented the fast decay of fluorescence of myofibrils on silver mirrors (arrow). It was best fitted by the four exponentials with lifetimes $\tau_1=0.029\pm0.001$, $\tau_2=0.215\pm0.006$, $\tau_3=1.077\pm0.017$, and $\tau_4=3.318\pm0.028$ ns; and the relative contributions to the total amplitude of 88.66, 7.81, 2.52, and 1.01%, respectively. The amplitude weighted average lifetime decreased 34 times to 0.068 ns.

3.4 Decrease of Bleaching in SMD Experiments

The signal from a sarcomere of a myofibril was measured by positioning an O-band by a piezostage over the projection of the confocal aperture on the sample plane as described in Ref. 18.

3.4.1 Glass+SIF

The intensity of myofibrils on glass was increased by SIF alone, four to five on average, times (Table 1). The decay on glass coverslips was best fitted by quickly and slowly decaying exponentials with the average contribution to the total intensity of $\alpha_1=23$ and $\alpha_2=77\%$. The decay in the presence of SIF was best fitted by quickly and slowly decaying exponentials with the average contributions to the total intensity of $\alpha_1=36\%$ and $\alpha_2=64\%$. In 12 separate experiments, SIF caused the average short half-time of myofibrils on plain coverslips to increase from 20 ± 4 to 25 ± 4 s [mean ± standard error (SE)]. The long half-time could not be reliably fitted. These results confirm the results of earlier experiments showing that photobleachings on glass were showed down by SIF only a little.[2] The results are summarized in Table 3.

3.4.2 Gold+SIF

The intensity of myofibrils on the gold mirror coated with SIF increased on average 10 times in comparison with uncoated glass (Table 1). Figure 6(A) compares photobleaching of the O-band of myofibrils on gold mirrors (green) with myofibrils on gold mirrors coated with SIF (red). The decay on gold

mirrors was best fitted by quickly and slowly decaying exponentials with the average contributions to the total intensity of $\alpha_1=32$ and $\alpha_2=68\%$. The decay on gold mirrors coated with SIF was best fitted by quickly and slowly decaying exponentials with the average contributions to the total intensity of $\alpha_1=26\%$ and $\alpha_2=74\%$. In six separate experiments, SIF caused the average short half-time of myofibrils on gold mirrors to increase $f_1=1.6$-fold from 19 ± 2 to 30 ± 6 s. The long half-time increased $f_2=2.9$-fold from 89 ± 4 to 260 ± 39 s. The results are summarized in Table 3. These results show that coating gold mirrors with SIF decreased fast photobleaching on average 2.5-fold ($\alpha_1^{\text{aver}}f_1+\alpha_2^{\text{aver}}f_2$, where α_1^{aver} and α_2^{aver} are the average change in α on the addition of SIF).

3.4.3 Silver+SIF

The intensity of myofibrils on silver mirror coated with SIF increased on average 259 times in comparison with uncoated glass (Table 1). Figure 6(B) compares photobleaching of the O-band of myofibrils on a silver mirror (green) with myofibrils on a silver mirror coated with SIF (red). The decay on the silver mirror was best fitted by quickly and slowly decaying exponentials with the average contributions to the total intensity of $\alpha_1=40\%$ and $\alpha_2=60\%$. The decay on the silver mirrors coated with SIF was best fitted by quickly and slowly decaying exponentials with the average contributions to the total intensity of $\alpha_1=41\%$ and $\alpha_2=59\%$. In 10 separate experiments, SIF caused the average short half-time of myofibrils on silver mirrors to increase on average $f_1=2.5$-fold from $\tau_1=21\pm2$ to $\tau_1=52\pm8$ s. The long half-time increased on average $f_2=2.5$ fold from $\tau_2=80\pm4$ to $\tau_2=202\pm6$ s. The results are summarized in Table 3. These results show that coating silver mirrors with SIF decreased photobleaching on average 2.5-fold.

3.4.4 Aluminum and Aluminum+SIF

The intensity of myofibrils on aluminum mirror coated with SIF increased on average 13 times in comparison with uncoated glass (Table 1). Photobleaching of the O-band of myofibrils on aluminum mirrors and on a mirror coated with SIF was best fitted by quickly and slowly decaying exponentials with the average contributions to the total intensity of $\alpha_1=42\%$ and $\alpha_2=58\%$. The decay on the aluminum mirrors was best fitted by quickly and slowly decaying exponentials with the average contributions to the total intensity of $\alpha_1=43\%$ and $\alpha_2=57\%$. In 12 separate experiments, SIF caused the average short half-time of myofibrils on aluminum mirrors to increase on average $f_1=2.1$-fold from $\tau_1=19\pm7$ to $\tau_1=40\pm5$ s. The long half-time increased on average $f_2=3.4$-fold from $\tau_2=40\pm6$ to $\tau_2=136\pm24$ s. The results are summarized in Table 3. These results show that coating aluminum mirrors with SIF decreased photobleaching on average 2.9-fold.

4 Discussion

The proximity of fluorophores to metallic particles provides an opportunity to increase and manipulate radiative rate.[20] In
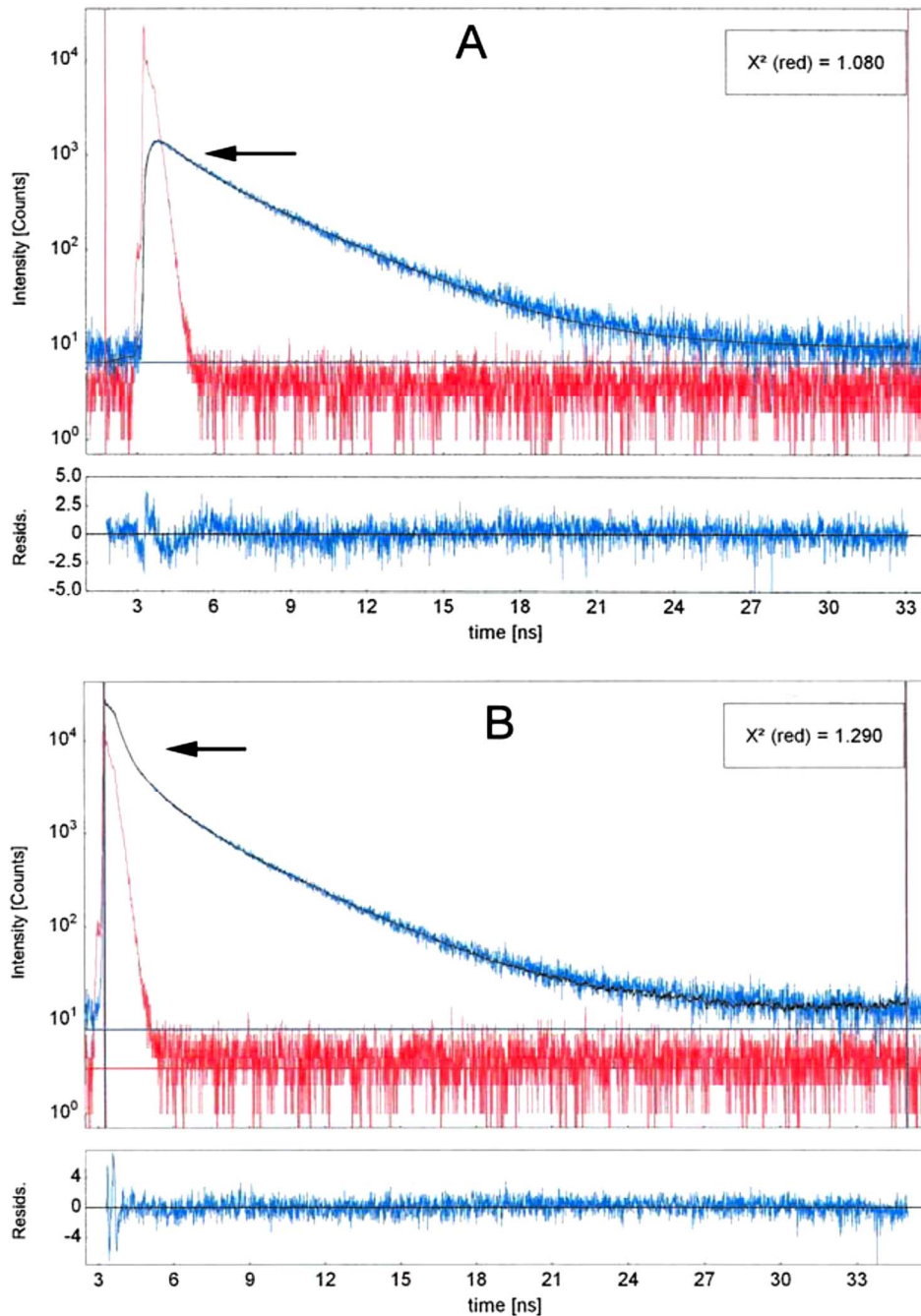
Fig. 5 Decrease of lifetime caused by SIF on silvered glass. (a) Lifetime signal from myofibrils on silver-covered glass (blue) is best fitted (black line) by the two exponentials with lifetimes $\tau_1 = 0.936 \pm 0.064$ and $\tau_2 = 3.380 \pm 0.041$ ns and with the relative contributions to the total amplitude of 43.05 and 56.95. The red signal is the exciting pulse. The bottom inset is the residual fit to all 7831 analyzed data points. (b) Lifetime signal from myofibrils on silver-covered glass coated with SIF (blue) is best fitted (black line) by four exponentials with lifetimes $\tau_1 = 0.029 \pm 0.000$, $\tau_2 = 0.215 \pm 0.006$, $\tau_3 = 1.077 \pm 0.017$, and $\tau_4 = 3.318 \pm 0.028$ ns and with the relative contributions to the total amplitude of 88.66, 7.81, 2.52, and 1.01%. The arrow points to the fast decay of fluorescence. The red signal is the exciting diode laser pulse. The bottom graph is the residual fit to all 7924 data points analyzed. (Color online only.)

addition to the trivial reflection from the mirror, the observed enhancement of fluorescence is probably due to enhanced near-field interactions between LSPs, which lead to a significant increase of the spontaneous radiative rate of a fluorophore. Such enhancement is well known in SPR signals.[21] In contrast to conventional enhancement of fluorescence, which

is always due to decrease of nonradiative rate constant and results in the increase of fluorescence lifetime,[22] the increase in radiative rate causes a decrease in lifetime. Such a decrease was indeed observed here. The effect of SIF was most dramatic when the relative contributions of the fast-slow and slow decays were considered. There was no picosecond decay

Table 3 Effect of SIF on the half-time of photobleaching (mean±SE).

| | Half-Time of Photobleaching (s) | | | |
| | −SIF | | +SIF | |
Substrate	τ_1	τ_2	τ_1	τ_2
Glass	20±4	88±1	25±4	CNF
Au[a]	19±2	89±4	30±6	260±39
Ag[a]	21±2	80±4	52±8	202±6
Al[a]	19±7	40±6	40±5	136±24

[a]Metal on glass.

CNF, Could not be fitted.

on glass, whereas on SIF it constituted ∼94% of the amplitude. The slow component constituted ∼60% of the decay amplitude on glass, whereas on SIF it constituted only ∼1.5% of the amplitude. The effect was most dramatic on silver mirrors. The intensity was enhanced 72-fold by SIF in comparison with the intensity on silver mirror, and 259-fold in comparison with the intensity on glass alone. The fast component on the silver mirror increased from 43 to 89% on SIF; the slow component decreased from 56 to 1.0% on SIF. Note that the shape of the spectra of the dye are not significantly altered by SIF (Fig. 3).

The combined effect of enhancement of brightness and lifetime decrease was to decrease photobleaching. The decrease in lifetime decreased the photobleaching because the probability of oxygen attack during the time a molecule was in the exited state was minimized.

We observed earlier that the reduction of photobleaching by SIF became significant only when myofibrils were placed on a high-refractive-index surface.[2] However, the uses of high-refractive-index (sapphire-based) coverslips have two disadvantages. First, they are expensive (they cannot be reused after coating with SIF). Second, they require the use of rapidly drying and toxic high-index-of-refraction (1.78) immersion oil. In this work, the decrease in photobleaching was observed while myofibrils were on glass. In contrast to the earlier work,[2] here we used direct sample illumination. Although this makes it impossible to illuminate a sample with a total internal reflection (TIR) evanescent wave, it has the advantages that myofibrils can be observed on substrates that are nearly completely opaque, and that myofibrils can be placed on thick microscope slides that are not as fragile as coverslips and thus easier to coat with SIF.

To explain such great enhancement in fluorescence and photostability for fluorophores, as observed here, we propose a simple model. The silver mirror acting together with silver islands may have two different consequences. The first consequence is due to the fact that the silver islands, and thereby the fluorophores, interact with their mirror images. This means the electric field at the fluorophores is at least doubled, and that the radiation from the fluorophores is superimposed by their mirror images. The intensity at the fluorophores is therefore at least quadrupled and so is the radiation. Alto-
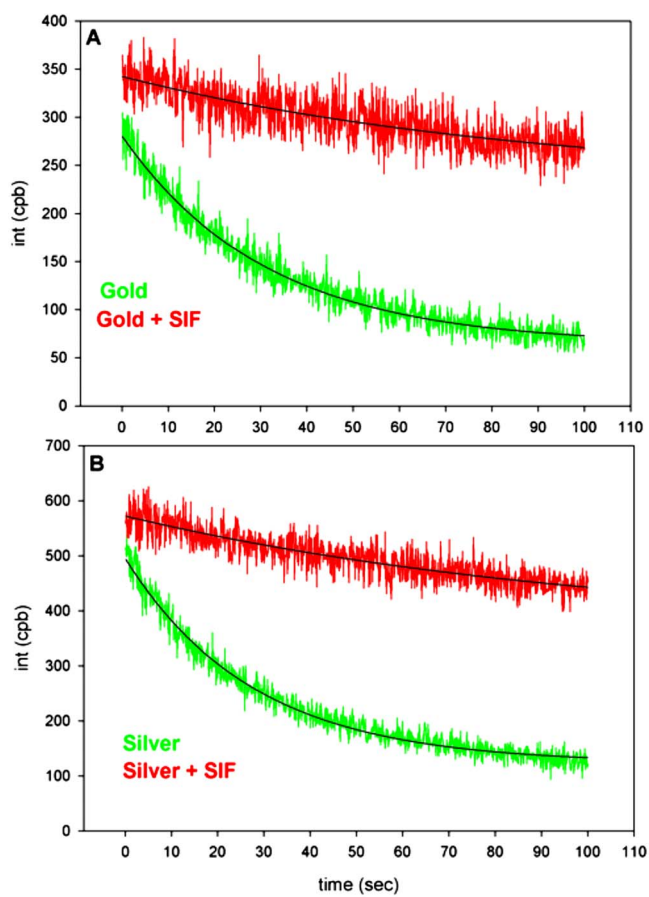

Fig. 6 Comparison of the rate of photobleaching of myofibrillar overlap zone on SIF on metal (red) and on plain metal (green). Myofibrils (1 mg/mL) were labeled with 0.01 μM rhodamine-phalloidin +9.99 μM unlabeled phalloidin. The overlap zone of a myofibril was viewed by SMD microscopy through a 4-μm confocal aperture. The three-parameter single exponential fits are in black. NA=1.45 objective. CPB denotes counts per 100-ms bin. Signal on (a) gold surface with SIF signal is attenuated 2.5 times and (b) on silver surface. SIF signal is first attenuated threefold using a two-exponential fit and another 50-fold using a three-parameter single-exponential fit. (Color online only.)

gether, this gives a factor of at least 16 for the enhancement under perfect conditions. This is illustrated in the top panel of Fig. 7. The other, perhaps dominant consequence, is due to near-field interaction of the silver islands mediated by surface plasmons at the silver mirror. In a simple approximation the oscillating dipoles interact as $1/r^3$ for small r and as $1/r$ for large r, where r is the separation between dipoles. For a 2D dipole assembly in close proximity to a suitable surface, the interaction between the dipoles would go via a surface mode as $\exp(-\alpha r)/\sqrt{r}$, where α depends on the propagation length of that mode. We estimate that surface plasmons at the silver mirror may propagate up to 10 μm and therefore couple strongly a large number of dipoles, i.e., silver islands. This results in a large enhancement effect,[23–25] as is illustrated in the bottom panel of Fig. 7.

5 Conclusions

The photobleaching phenomenon is exceedingly important in microscopy. Increased photostability enables longer exposure
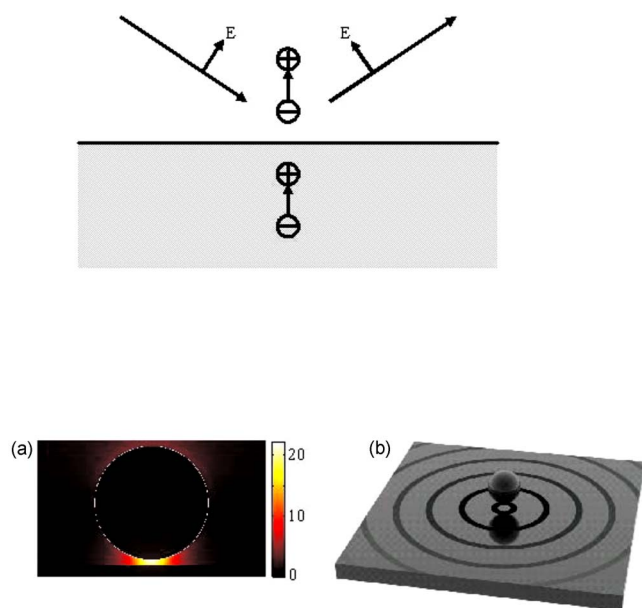
Fig. 7 Cause of SIF-induced enhancement. Top panel, the *E*-fields of the incident and reflected beams add, and so does the dipole moment with its mirror image. Bottom panel, (a) calculation of the electric field enhancement at a silver sphere above a silver mirror in the Rayleigh limit and (b) the particle (sphere) creates surface plasmons radiating from the sphere in two dimensions. The size of the sphere in comparison to the wavelength is greatly exaggerated in this figure; a large number of particles should be within one wavelength. Then they cooperate coherently. Particles more distant cooperate incoherently, i.e., the intensities, not amplitudes, are added.

times of the specimen to the impinging light. This, of course, results in more detailed images and enables accurately tracing the changes occurring in the observed objects. The method described here gives over two orders of magnitude stronger signals with well-preserved spectral properties of the fluorescent probe. The quality of images on SIF-coated surfaces still requires improvement.[5] We believe, however, that this can be overcome with a better-controlled deposition of silver nanoparticles (work in progress).

Acknowledgments

References

1. Z. Gryczynski, J. Borejdo, N. Calander, E. G. Matveeva, and I. Gryczynski, "Minimization of detection volume by surface plasmon-coupled emission," *Anal. Biochem.* **356**, 125–131 (2006).
2. J. Borejdo, Z. Gryczynski, N. Calander, P. Muthu, and I. Gryczynski, "Application of surface plasmon coupled emission to study of muscle," *Biophys. J.* **91**, 2626–2635 (2006).
3. M. Velez and D. Axelrod, "Polarized fluorescence photobleaching recovery for measuring rotational diffusion in solutions and membranes," *Biophys. J.* **53**(4), 575–591 (1988).
4. Y. Harada, K. Sakurada, T. Aoki, D. D. Thomas, and T. Yanagida, "Mechanochemical coupling in actomyosin energy transduction studied by *in vitro* movement assay," *J. Mol. Biol.* **216**, 49–68 (1990).
5. P. Muthu, I. Gryczynski, Z. Gryczynski, J. Talent, I. Akopova, K. Jain, and J. Borejdo, "Decreasing photobleaching by silver island films: application to muscle," *Anal. Biochem.* (in press).
6. S. Hayashi, "Spectroscopy of gap modes in metal particle-surface systems," in *Topics in Applied Physics, Near Field Optics and Surface Plasmon Polaritons*, S. Kawata, Ed., Vol. **81**, pp. 71–95, Springer-Verlag (2001).
7. E. G. Matveeva, I. Gryczynski, A. Barnett, Z. Leonenko, J. R. Lakowicz, and Z. Gryczynski, "Metal particle-enhanced fluorescent immunoassays on metal mirrors," *Anal. Biochem.* **363**(2), 239–245 (2007).
8. E. Hutter and J. H. Fendler, "Exploitation of localized surface plasmon resonance," *Adv. Mater. (Weinheim, Ger.)* **16**, 1685–1706 (2004).
9. J. R. Lakowicz, Y. Shen, S. D'Auria, J. Malicka, J. Fang, Z. Gryczynski, and I. Gryczynski, "Radiative decay engineering. 2. Effects of silver island films on fluorescence intensity, lifetimes, and resonance energy transfer," *Anal. Biochem.* **301**, 261–277 (2002).
10. D. A. Weitz, S. Garoff, C. D. Anson, and T. J. Gramila, "Fluorescent lifetimes of molecules on silver-island films," *Opt. Lett.* **7**, 89–91 (1982).
11. A. Leitner, M. E. Lippitch, S. Draxler, M. Riegler, and F. R. Aussenegg, "Fluorescence properties of dyes absorbed to silver islands, investigated by picosecond techniques," *Appl. Phys. B* **36**, 105–109 (1985).
12. I. Gryczynski, J. Malicka, Y. Shen, Z. Gryczynski, and J. R. Lakowicz, "Multiphoton excitation of fluorescence near metallic particles: enhanced and localized excitation," *J. Phys. Chem. B* **106**, 2191–2195 (2002).
13. B. P. Maliwal, J. Malicka, I. Gryczynski, Z. Gryczynski, and J. R. Lakowicz, "Fluorescence properties of labeled proteins near silver colloid surfaces," *Biopolymers* **70**(4), 585–594 (2003).
14. C. D. Geddes, H. Cao, I. Gryczynski, Z. Gryczynski, and J. R. Lakowicz, "Metal-enhanced fluorescence (MEF) due to silver colloid on a planar surface: potential applications of indocyanine green to *in vivo* imaging," *J. Phys. Chem. A* **107**, 3443–3449 (2003).
15. J. Malicka, I. Gryczynski, and J. R. Lakowicz, "DNA hybridization assays using metal-enhanced fluorescence," *Biochem. Biophys. Res. Commun.* **306**(1), 213–218 (2003).
16. J. Malicka, I. Gryczynski, J. Fang, and J. R. Lakowicz, "Photostability of Cy3 and Cy5-labeled DNA in the presence of metallic silver particles," *J. Fluoresc.* **12**, 439–447 (2002).
17. K. H. Drexhage, in *Progress in Optics*, E. Wolfe, pp. 161–232, North Holland, Amsterdam (1974).
18. J. Borejdo, N. Calander, Z. Gryczynski, and I. Gryczynski, "Fluorescence correlation spectroscopy in surface plasmon coupled emission microscope," *Opt. Express* **14**(17), 7878–7888 (2006).
19. J. Borejdo, P. Muthu, J. Talent, I. Akopova, and T. P. Burghardt, "Rotation of actin monomers during isometric contraction of skeletal muscle," *J. Biomed. Opt.* **12**, 014013 (2007).
20. J. R. Lakowicz, J. Malicka, I. Gryczynski, Z. Gryczynski, and C. D. Geddes, "Radiative decay engineering: the role of photonic mode density in biotechnology," *J. Phys. D* **36**, R240–R249 (2003).
21. M. J. Natan and A. L. Lyon, "Surface plasmon resonance biosensing with colloidal Au amplification," in *Metal Nanoparticles*, D. I. Feldheim and C. A. Foss, Eds., pp. 183–205, Marcel Dekker, New York (2002).
22. J. R. Lakowicz, *Principles of Fluorescence Spectroscopy*, Springer (2006).
23. H. R. Stuart and D. G. Hall, "Enhanced dipole-dipole interaction between elementary radiators near a surface," *Phys. Rev. Lett.* **80**(25), 5663–5666 (1998).
24. N. Felidj, J. Aubard, and G. Levi, "Enhanced substrate-induced coupling in two-dimensional gold nanoparticle arrays," *Phys. Rev. B* **66**, 245407 (2002).
25. J.-H. Song, T. Atay, S. Shi, H. Urabe, and A. V. Nurmikko, "Large enhancement of fluorescence efficiency from CdSe/ZnS quantum dots induced by resonant coupling to spatially controlled surface plasmons," *Nano Lett.* **5**(8), 1557–1561 (2005).